Cell

PI(4,5)P_2-Dependent and Ca^{2+}-Regulated ER-PM Interactions Mediated by the Extended Synaptotagmins

Francesca Giordano,[1,3,4,7] Yasunori Saheki,[1,3,4,7] Olof Idevall-Hagren,[1,3,4] Sara Francesca Colombo,[5] Michelle Pirruccello,[1,3,4] Ira Milosevic,[1,3,4] Elena O. Gracheva,[2,3] Sviatoslav N. Bagriantsev,[2] Nica Borgese,[5,6] and Pietro De Camilli[1,3,4,*]

[1]Department of Cell Biology
[2]Department of Physiology
[3]Program in Cellular Neuroscience, Neurodegeneration, and Repair
[4]Howard Hughes Medical Institute
Yale School of Medicine, New Haven, CT 06510, USA
[5]CNR Institute of Neuroscience and BIOMETRA Department, Università degli Studi di Milano, 20129 Milan, Italy
[6]Department of Health Science, Magna Graecia University of Catanzaro, 88100 Catanzaro, Italy
[7]These authors contributed equally to this work
*Correspondence: pietro.decamilli@yale.edu
http://dx.doi.org/10.1016/j.cell.2013.05.026

SUMMARY

Most available information on endoplasmic reticulum (ER)-plasma membrane (PM) contacts in cells of higher eukaryotes concerns proteins implicated in the regulation of Ca^{2+} entry. However, growing evidence suggests that such contacts play more general roles in cell physiology, pointing to the existence of additionally ubiquitously expressed ER-PM tethers. Here, we show that the three extended synaptotagmins (E-Syts) are ER proteins that participate in such tethering function via C2 domain-dependent interactions with the PM that require PI(4,5)P_2 in the case of E-Syt2 and E-Syt3 and also elevation of cytosolic Ca^{2+} in the case of E-Syt1. As they form heteromeric complexes, the E-Syts confer cytosolic Ca^{2+} regulation to ER-PM contact formation. E-Syts-dependent contacts, however, are not required for store-operated Ca^{2+} entry. Thus, the ER-PM tethering function of the E-Syts (tricalbins in yeast) mediates the formation of ER-PM contacts sites, which are functionally distinct from those mediated by STIM1 and Orai1.

INTRODUCTION

The endoplasmic reticulum (ER) forms a complex network that extends throughout the cell and plays a multiplicity of functions, including protein synthesis, lipid metabolism, and Ca^{2+} storage for intracellular signaling. Although membranes of the ER are functionally connected to all membranes of the secretory and endocytic pathways via vesicular transport, they only fuse with each other and with vesicles involved in retrograde transport from the Golgi complex. However, there is growing evidence that close appositions between the ER and the membranes of virtually all other membranous organelles play major roles in cell physiology. These sites are thought to be involved in exchanges of molecules, such as lipids, in the function of ER-localized enzymes that act "in trans" on the apposed membrane and in the control of Ca^{2+} homeostasis (Elbaz and Schuldiner, 2011; Friedman and Voeltz, 2011; Holthuis and Levine, 2005; Stefan et al., 2011, 2013; Toulmay and Prinz, 2011).

In cells of higher eukaryotes, ER-plasma membrane (PM) contact sites were first described by electron microscopy in the 1950s in muscle (Porter and Palade, 1957), where they are extremely abundant. They were subsequently observed also in neurons (Rosenbluth, 1962). More recently, it has become clear that they represent a general feature of all eukaryotic cells, although, due to their small size in most cells, they are frequently overlooked in electron micrographs (Friedman and Voeltz, 2011).

A well-established function of ER-PM junctions in metazoan cells is control of Ca^{2+} dynamics. In muscle, they are responsible for depolarization-contraction coupling (Endo, 2009), as they are sites where the juxtaposition of voltage-dependent Ca^{2+} channels in the PM and ryanodine receptors in the ER membrane couple Ca^{2+} entry from the extracellular space to Ca^{2+} release from the ER (Block et al., 1988; Franzini-Armstrong and Jorgensen, 1994; Takeshima et al., 2000). ER-PM contact sites are also responsible for store-operated Ca^{2+} entry (SOCE). Oligomerization of the ER protein STIM1 in response to lowered Ca^{2+} levels in the ER lumen triggers its interaction with, and activation of, the PM Ca^{2+} channel Orai1, leading to Ca^{2+} influx to restore normal Ca^{2+} levels in the ER (Feske et al., 2006; Lewis, 2007; Liou et al., 2005; Orci et al., 2009; Zhang et al., 2005). Although depletion of intracellular Ca^{2+} stores enhances areas of apposition between the PM and the ER, focal ER-PM contact sites exist before STIM1 recruitment (Orci et al., 2009; Shen et al., 2011). This is consistent with the presence of ER-localized enzymes expected to act in trans on PM substrates (Anderie et al., 2007; Stefan et al., 2011) and of ER proteins (VAP-A and VAP-B) that bind

PM-interacting proteins (Levine and Loewen, 2006; Schulz et al., 2009). However, neither these ER enzymes nor VAP family proteins are selectively localized at ER-PM contacts, speaking against their specialized role in the generation of such sites.

In yeast, where some of the metabolic functions requiring direct ER to PM apposition have been characterized (Holthuis and Levine, 2005; Stefan et al., 2011), the bulk of the ER (more than 50%) has a cortical localization (West et al., 2011). Thus, studies of proteins that mediate cortical ER formation in yeast may help elucidate the most fundamental properties of ER-PM contacts. Recently, three yeast ER proteins, the tricalbins (Tcb1p, Tcb2p, and Tcb3p), were shown to be selectively concentrated in the cortical ER and to play a key role in ER-PM tethering (Manford et al., 2012; Toulmay and Prinz, 2012). Tricalbins are ER integral membrane proteins with a cytosolic synaptotagmin-like mitochondrial lipid binding protein (SMP) domain followed by multiple C2 domains (Creutz et al., 2004; Lee and Hong, 2006). SMP domains, which are lipid-binding modules, are proposed to have specialized function at membrane contact sites, possibly in lipid exchange between the two membranes (Kopec et al., 2010; Toulmay and Prinz, 2012). C2 domains are generally acidic phospholipid-binding modules and thus have the potential to bind the PM in trans (Rizo and Südhof, 1998). Mammalian cells express three proteins that share sequence and domain similarity to the tricalbins, the extended synaptotagmins (E-Syt1, E-Syt2, and E-Syt3) (Lee and Hong, 2006; Min et al., 2007). Based on the expression of epitope-tagged constructs in mammalian cells, E-Syt1 was reported to localize in an undetermined intracellular compartment, whereas E-Syt2 and E-Syt3 were reported to localize to the PM (Min et al., 2007).

We have now found that all three E-Syts are ER-anchored proteins. They form homo- and heteromeric complexes that mediate contacts with the PM. Such contacts are critically dependent on the presence of $PI(4,5)P_2$ in this membrane and are additionally regulated by cytosolic Ca^{2+} via the Ca^{2+}-sensing property of E-Syt1. As they are not required for SOCE, they are functionally distinct from the STIM1-induced contacts.

RESULTS

E-Syts Localize to the ER, and Their Overexpression Induces Cortical ER

The subcellular targeting of each E-Syt protein was analyzed by transfecting cells with tagged constructs whose expression was confirmed by western blotting (none of the available antibodies produced a specific immunocytochemical signal). To rule out artifacts due to tag-induced mistargeting, multiple constructs were used, including E-Syts tagged with EGFP or mCherry at the N or C terminus or with small N- or C-terminal tags (Myc or FLAG) (Figure 1 and Figure S1 available online). In the following text, the position of the tag name relative to the protein name indicates its N- or C-terminal location, respectively. All constructs yielded similar results. As previously described using the same approach (expression of tagged constructs) (Min et al., 2007), E-Syt1 had a broad intracellular distribution, while E-Syt2 and E-Syt3 had a predominant PM-like localization, although in some cells, we detected a substantial intracellular pool of E-Syt2 (Figures 1B, S1B–S1D, S1H, and S1K). E-Syt1 colocalized with the cotransfected ER marker Sec61β fused to monomeric red fluorescent protein (mRFP) (mRFP-Sec61β) (Shibata et al., 2008), indicating a localization throughout the ER (Figures 1B, S1A, and S1G). Although E-Syt2 and E-Syt3 had a very different localization from E-Syt1, their expression, which resulted in overexpression relative to the endogenous proteins (Figure S1E), shifted a pool of mRFP-Sec61β to the cell periphery, where it colocalized with E-Syt2 and E-Syt3 (insets of Figure 1B). When present, the noncortical pool of E-Syt2 also colocalized with Sec61β (Figures S1B and S1H). A cortical shift of a pool of mRFP-Sec61β was also observed in cells overexpressing untagged E-Syt2 and E-Syt3, further excluding tag-induced artifacts (Figure S1F).

To determine whether the Sec61β signal overlapping with E-Syt2 and E-Syt3 at the cell periphery represented cortical ER, HeLa cells overexpressing E-Syt2 or E-Syt3 with or without a C-terminal EGFP tag were examined by electron microscopy. Some cells used for this analysis were additionally transfected with horseradish peroxidase (HRP) tagged with an ER retention motif (ssHRP-KDEL) (Schikorski et al., 2007), so that the ER could be identified via an electron dense (dark) HRP reaction product. In control cells, contacts between the ER-PM contacts were generally few in individual sections and small in size (Figures 1C and 7A). However, in cells overexpressing E-Syt2, and even more so in cells overexpressing E-Syt3, a massive presence of ER elements closely apposed to the PM via a ribosome-free surface (average distance of 10 ± 3 nm) was observed (arrows in Figures 1D–1H).

E-Syt2 and E-Syt3 Localize at Sites of Apposition between the ER and the PM

The ability of E-Syt2 and E-Syt3 to induce cortical ER suggests that they directly participate in bridging the two membranes. If so, they should be localized at the interface of the two membranes. To test this hypothesis, anti-EGFP-immunogold electron microscopy (EM) (10 nm gold) was performed on ultrathin frozen sections of E-Syt-EGFP expressing HeLa cells. Consistent with fluorescence imaging, E-Syt2-EGFP (Figure 1I) and E-Syt3-EGFP (Figure 1J) were highly concentrated at the expanded areas of apposition between the PM and the ER, which were identified by coimmunolabeling (5 nm gold) for endogenous protein disulfide isomerase (PDI), a resident lumenal protein of the ER. No immunogold was observed on regions of the PM not in contact with the ER (Figures 1I and 1J). In agreement with fluorescence imaging, E-Syt1-EGFP was broadly detected on ER elements throughout the cell (arrows, Figure 5C). Notably, however, at the few and small ER-PM contacts visible in these cells, anti-E-Syt1-EGFP immunogold was frequently observed (arrowhead in Figure 5C).

Subcellular Targeting of the E-Syts and Synaptotagmin 1 Is Distinct

A selective localization of the E-Syts in the ER contrasts with the predominant localization of the ''bona fide'' synaptotagmins in post-Golgi membranes (Südhof, 2002, 2012). Synaptotagmin 1 (Syt1), the founding member of the synaptotagmin family, is localized primarily on synaptic and neurosecretory vesicles in neuronal cells (Perin et al., 1990) and primarily at the PM in non-neuronal cells due to absence in these cells of a specific adaptor

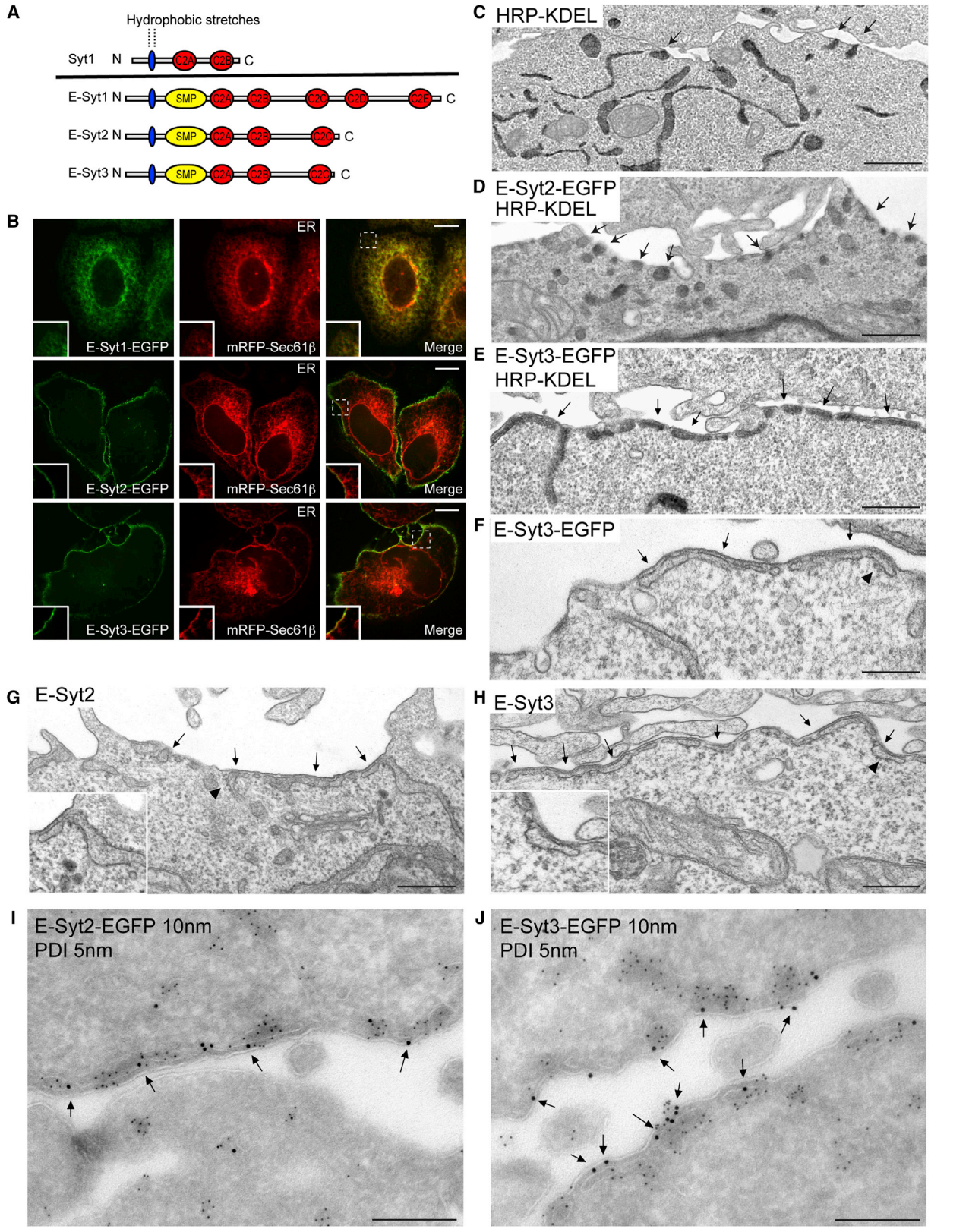

(legend on next page)

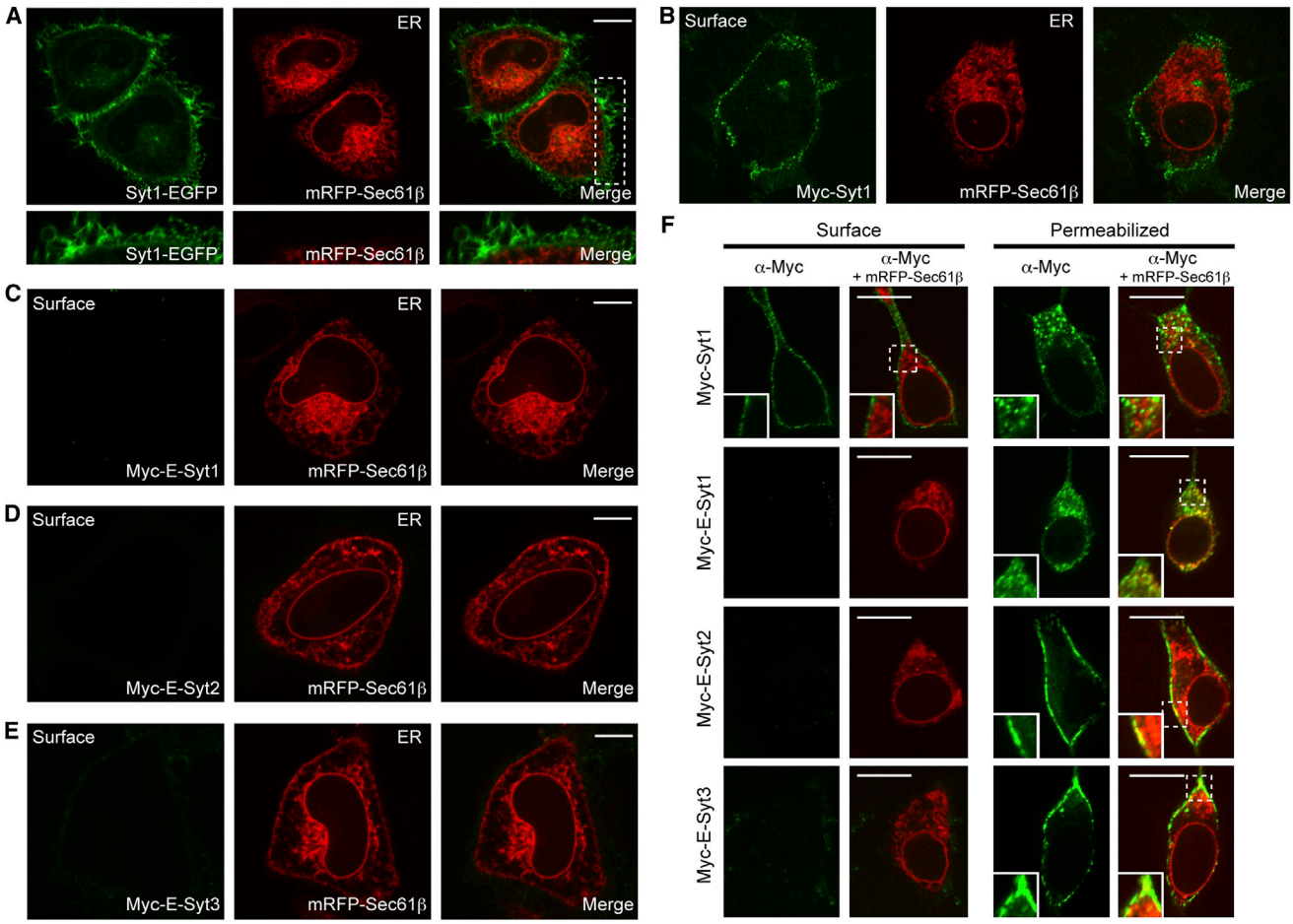

Figure 2. Comparison of the Accessibility of the N Termini of Syt1 and of the E-Syts to the Extracellular Space

(A) Confocal images of live HeLa cells expressing Syt1-EGFP and mRFP-Sec61β showing the predominant PM localization of Syt1 in these cells. Bottom images: high power view of the region outlined by dotted lines in the merge field.

(B–E) Fluorescent images of HeLa cells coexpressing mRFP-Sec61β and Myc-Syt1 or Myc-E-Syts as indicated and incubated with anti-Myc antibodies. The Myc epitope was accessible in the case of Myc-Syt1 but not in the case of Myc-E-Syts.

(F) Fluorescent images of SH-SY5Y neuroblastoma cells coexpressing mRFP-Sec61β (red) with either Myc-Syt1 or Myc-E-Syts (green) and incubated with anti-Myc antibodies before fixation (left panels, "surface") or after fixation and permeabilization (right panel, "permeabilized").

See also Figures S1 and S2.

needed for its endocytic recycling (Diril et al., 2006; Figures 2A, 2B, and 2F). The retention of the E-Syts in the ER was unexpected in view of the overall similarities between the two protein families: a single "predicted" transmembrane region preceded by a short amino acid sequence and followed by a large cytosolic domain comprising C2 domains. Thus, we performed a direct comparison, under the same conditions, of the subcellular targeting of the E-Syts and of Syt1.

In HeLa cells Syt1-EGFP produced an uninterrupted decoration of the PM, including its filopodia (Figure 2A). This fluorescent

Figure 1. Localization of the E-Syts in the ER and of E-Syt2 and E-Syt3 at ER-PM Contact Sites

(A) Domain structure of Syt1 and of the E-Syts.

(B) Confocal images of HeLa cells expressing E-Syt-EGFP fusions and the ER marker mRFP-Sec61β. Insets show at higher magnification the colocalization throughout the ER for E-Syt1 but only colocalization with the ER marker at the cell periphery for E-Syt2 and E-Syt3. Scale bar, 10 μm.

(C–H) Electron micrographs of HeLa cells transfected with the ER lumenal marker HRP-KDEL alone (C) or together with E-Syt2-EGFP (D) or E-Syt3-EGFP (E). Cells singly transfected with E-Syt3-EGFP (F), untagged E-Syt2 (G), or untagged E-Syt3 (H). The ER can be identified via an electron dense (dark) HRP reaction product in (C)–(E) and by presence of ribosomes (arrowheads) in (F)–(H). Arrows in (C)–(H) indicate cortical ER. Scale bar, 250 nm.

(I and J) Electron micrographs of ultrathin cryosections of HeLa cells transfected with E-Syt2-EGFP (I) or E-Syt3-EGFP (J) and double immunogold labeled for EGFP (10 nm gold) to detect E-Syts and for endogenous PDI (5 nm gold) to label the ER lumen. E-Syt2 and E-Syt3 are almost exclusively localized to the cortical ER (arrows). Scale bar, 200 nm.

See also Figure S1.

pattern was different from the somewhat discontinuous PM lining of E-Syt2 and E-Syt3 that did not extend into the filopodia (compare with Figure 1B). Furthermore, when a small N-terminal Myc-tag was added to Syt1, the tag could be detected at the cell surface in nonfixed, nonpermeabilized HeLa cells kept at 4°C (Figure 2B). In contrast, no signal of identically N-terminally Myc-tagged E-Syts was detected at the cell surface under these conditions (Figures 2C–2E). Similarly, surface accessibility of Syt1 and nonaccessibility of the E-Syts were observed in SH-SY5Y neuroblastoma cells (Figure 2F). In these cells, an additional punctate localization of Syt1 that did not colocalize with the ER marker Sec61β could be observed in the cytoplasm after fixation and Triton X-100 permeabilization, as expected for secretory vesicle localization. In contrast, the localization of the E-Syts, as revealed by anti-Myc antibodies following fixation and permeabilization, was the same as that observed in non-neuronal cells: a localization that globally overlaps with that of the cotransfected Sec61β for E-Syt1 and a cortical localization that only overlaps with a peripheral pool of Sec61β for E-Syt2 and E-Syt3 (Figures 2F).

E-Syts Associate with the ER Membrane Bilayer via a Hairpin Sequence

An additional difference between the E-Syts and Syt1 was revealed by the characterization of the topology of the E-Syts in the membrane. The E-Syts, like Syt1, were proposed to be integral membrane proteins with the N terminus localized in the noncytosolic space and a single transmembrane span originating from a type I signal-anchor sequence (Lee and Hong, 2006; Min et al., 2007; Toulmay and Prinz, 2012). In Syt1, which, like the E-Syts, lacks a signal sequence, the addition of a folded module (but not of a short epitope) to its N terminus prevents its translocation across the ER membrane (Kida et al., 2005). Accordingly, addition of an EGFP tag without a signal sequence to the N terminus of Syt1 disrupts its localization, resulting in large aggregates (Figure S1J). In contrast, E-Syts harboring folded modules (EGFP or mCherry) without a signal sequence at their N terminus had the same localization and intracellular dynamics as C-terminal tagged E-Syts (Figures S1G–S1I and S1K), raising the possibility that their N termini may not be translocated across the membrane. As only one potential membrane anchoring sequence is predicted in the E-Syts by hydrophilicity analysis (Figure S2J), the cytosolic location of both the N and C termini could be explained by a hairpin structure of this hydrophobic sequence.

Inspection of the putative transmembrane segments of all three E-Syts reveals that their length, 30 or 31 amino acids (Figure 3A), not only exceeds the length of the transmembrane region of the synaptotagmins (reported as 27 amino acids [aa] for synaptotagmin II; Kida et al., 2005) and of other proteins of post-Golgi membranes but, more importantly, exceeds that of the transmembrane regions of typical integral membrane proteins of the ER (on average about 20 aa) (Higy et al., 2004; Sharpe et al., 2010). This length is compatible with formation of a hairpin that penetrates but does not cross entirely the bilayer, as shown for the hydrophobic membrane stretches of several other ER proteins, such as the reticulons (Voeltz et al., 2006). The putative transmembrane domain of the yeast tricalbins has similar characteristics and is, in fact, slightly longer, with a charged amino acid in its center consistent with a hairpin spanning the entire bilayer (Figure 3A).

To determine whether the N termini of the E-Syts are exposed to the cytosol, the PM of cells coexpressing each N-terminally Myc-tagged E-Syt and the lumenal ER marker ER-mRFP was selectively permeabilized with low concentrations of digitonin (a treatment that does not permeabilize the ER membrane; Lorenz et al., 2006), and accessibility of the Myc epitopes was probed with fluorophore-conjugated anti-Myc antibodies without any fixation. While ER-mRFP was retained in the ER lumen, as expected (Figures S2Eand S2F), strong staining of the Myc epitopes was obtained under this condition (Figures 3B–3D), indicating that the N termini of all three E-Syts are accessible to the cytosolic surface of the ER.

Consistent with these findings, both the N-, C-terminally, and even internally linked fluorescent tags of E-Syts, like the C-terminally linked mCherry-tag of Sec61β (cytosolic mCherry, positive control), were accessible to protease K digestion, with total loss of fluorescence within 1 min upon digitonin treatment of nonfixed cells (Lorenz et al., 2006). In contrast, the fluorescence of VAP-A-EGFP (lumenal EGFP, negative control) was not affected (Figures S2A–S2I; Movies S1 and S2).

Finally, the mode of insertion of Syt1 and of an E-Syt was directly assessed by a cell-free translation-translocation assay (Brambillasca et al., 2005). When Myc-Syt1 and Myc-E-Syt3 were translated in the presence of rough microsomes, resistance to alkaline extraction demonstrated that both proteins became tightly integrated in the ER membrane (Figure S2L). This fits with the observation that endogenous E-Syt1, like other integral ER membrane proteins, such as calnexin and VAP-A, is resistant to alkaline and high salt extraction (Figure S2M). In the case of Myc-Syt1, an upward mobility shift of the translation product in the cell-free assay reflected utilization of an N-glycosylation site in the N-terminal region (abolished by the N-glycosylation tripeptide inhibitor [NYT]), thus demonstrating its translocation (Figure 3E, first three lanes). As E-Syt3 lacks an N-glycosylation consensus sequence, translocation was assessed by proteinase K protection of metabolically ($^{[35S]}$methionine) labeled proteins (see cartoon in Figure S2K). Anti-Myc immunoprecipitation followed by autoradiography revealed that a Myc-positive fragment was protected upon exposure of nonpermeabilized microsomes to proteinase K in the case of Myc-Syt1 but not in the case of Myc-E-Syt3, although the full-length products were immunoprecipitated with equal efficiency (Figure 3E). These results demonstrate the translocation of the N terminus of Myc-Syt1 but not Myc-E-Syt3.

Collectively, these results strongly support the hypothesis that the E-Syts are inserted in the ER through a hairpin sequence (Figure 3F).

Interaction of the C2C Domain of E-Syt2 and E-Syt3 with PM PI(4,5)P_2

A tethering function of E-Syt2 and E-Syt3 at the ER predicts that their cytosolically exposed domains bind in trans the PM. Their C2C domains (see Figure 1A for the nomenclature of the C2C domains) could contain such a binding site, as this domain

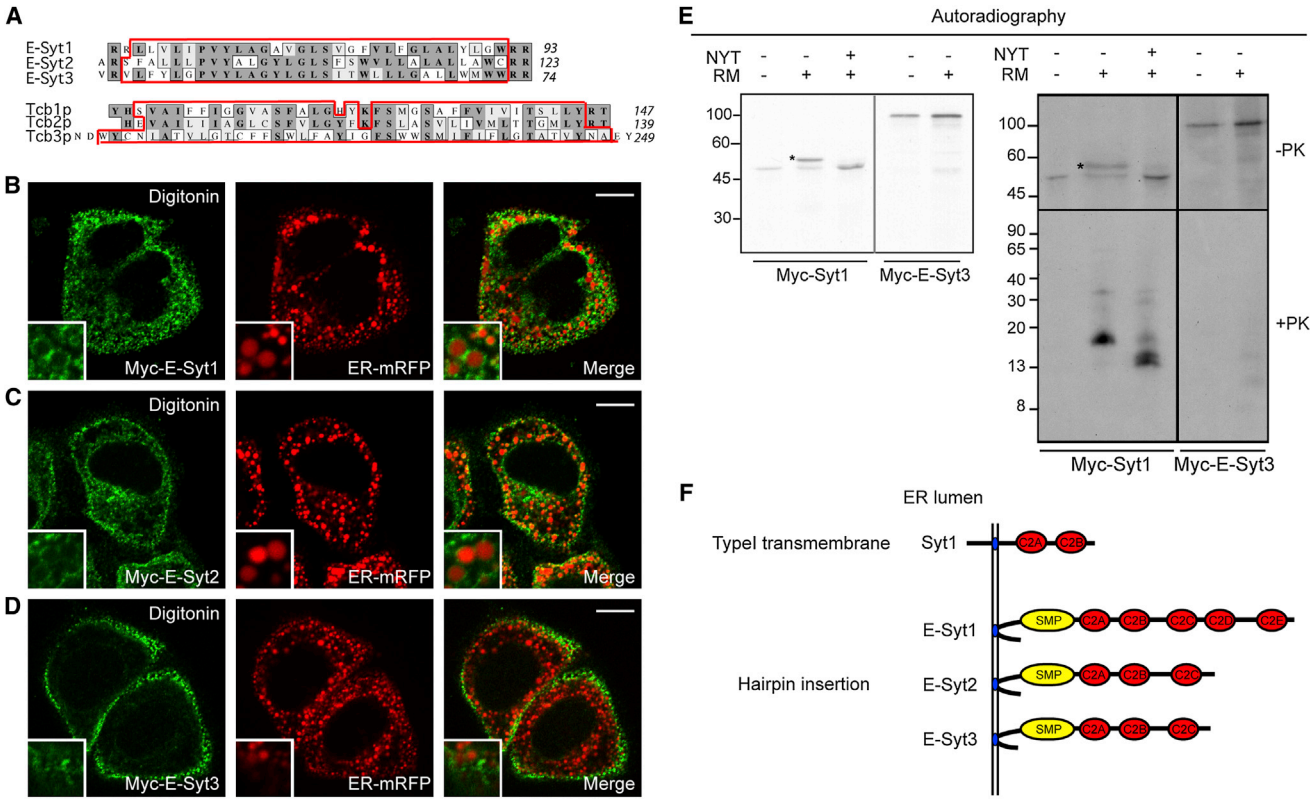

Figure 3. E-Syts Are Inserted into the ER Membranes via Hydrophobic Hairpin Sequences

(A) Alignments of putative transmembrane regions of the three E-Syts (human) and of the three tricalbins. The uncharged residues are contained in the red boxes. Conserved residues and substitutions are shaded in dark and light gray, respectively. The numbers on the right refer to the position of the last residue shown in each sequence.

(B–D) Fluorescence images of digitonin-permeabilized (20 μM) HeLa cells coexpressing Myc-E-Syts and ER-mRFP and incubated with Alexa Fluor 488-conjugated anti-Myc antibodies (green) before fixation, showing accessibility of N-terminal Myc epitopes at the surface of ER elements. At the concentration of digitonin used, ER membranes remain unpermeabilized although vesiculated due to cell lysis (see also Figure S2). Scale bar, 10 μm.

(E) Cell-free translation-translocation assays showing translocation across microsomal membranes of the N terminus of Syt1 but not of E-Syt3. (Left panel) Analysis of $^{[35S]}$Met-labeled Myc-Syt1 and Myc-E-Syt3 translated in vitro in the presence or absence of dog pancreas RM and NYT, as indicated. An asterisk indicates glycosylated Syt1. (Right panel) Results of protease protection assay. After translation, an aliquot of each fraction was immunoprecipitated with anti-Myc antibodies (top). A 10-fold larger aliquot of each sample was subjected to PK digestion before immunoprecipitation (bottom).

(F) Schematic cartoon showing the topology of Syt1 and of the E-Syts suggested by these experiments. The hydrophobic stretches (about 30 amino acids) previously predicted to cross the membrane are proposed to form hairpins in the ER bilayer.

See also Figure S2 and Movies S1 and S2.

was reported to be required for the peripheral localization (interpreted as a bona fide PM localization) localization of E-Syt2 and E-Syt3 (Min et al., 2007). Accordingly, E-Syt2 and E-Syt3 constructs lacking the C2C domain had a diffuse localization throughout the ER (Figures 4A, 4B, and S3B). Conversely, a deletion construct lacking the putative transmembrane region but containing the C2 domains (E-Syt2 C2ABC) (Figure 4I) and even the C2C domain alone (E-Syt2 C2C) (Figure 4B) were recruited to the PM, while a construct that lacks the SMP domain, E-Syt2 SMPΔ, was still recruited to cortical ER (Figure S3A).

C2 domains are phospholipid-binding modules, and for many of them, the interaction of a surface-exposed basic patch with acidic phospholipid bilayers is enhanced by PI(4,5)P_2 (Chapman, 2008; Fernandez et al., 2001; Rizo and Südhof, 1998), a phosphoinositide primarily concentrated in the PM (Di Paolo and De Camilli, 2006). The basic patch, but not the amino acids responsible for Ca^{2+} binding in a subset of C2 domains (Chapman, 2008; Fernandez et al., 2001), is present in the C2C domains of E-Syt2 and E-Syt3 (Figure S4A). Supporting a role of acidic phospholipids in E-Syt2 and E-Syt3 targeting, mutation of the basic residues (K805A, R806A, R807A, R810A, R811A, and K812A) responsible for the basic patch in the C2C domain of E-Syt2 abolished its cortical localization and resulted in a distribution of E-Syt2 throughout the ER (Figure 4B).

To directly test the role of PI(4,5)P_2 in E-Syt2 and E-Syt3 recruitment, we rapidly depleted this phosphoinositide in the PM using an optogenetic system recently developed in our lab. The system is based on the blue light-dependent heterodimerization of a cytosolically localized inositol 5-phosphatase domain with a PM-targeted module (Idevall-Hagren et al., 2012; Figure S3C).

COS-7 cells were cotransfected with (1) the two components of the heterodimerization system (CIBN-CAAX and

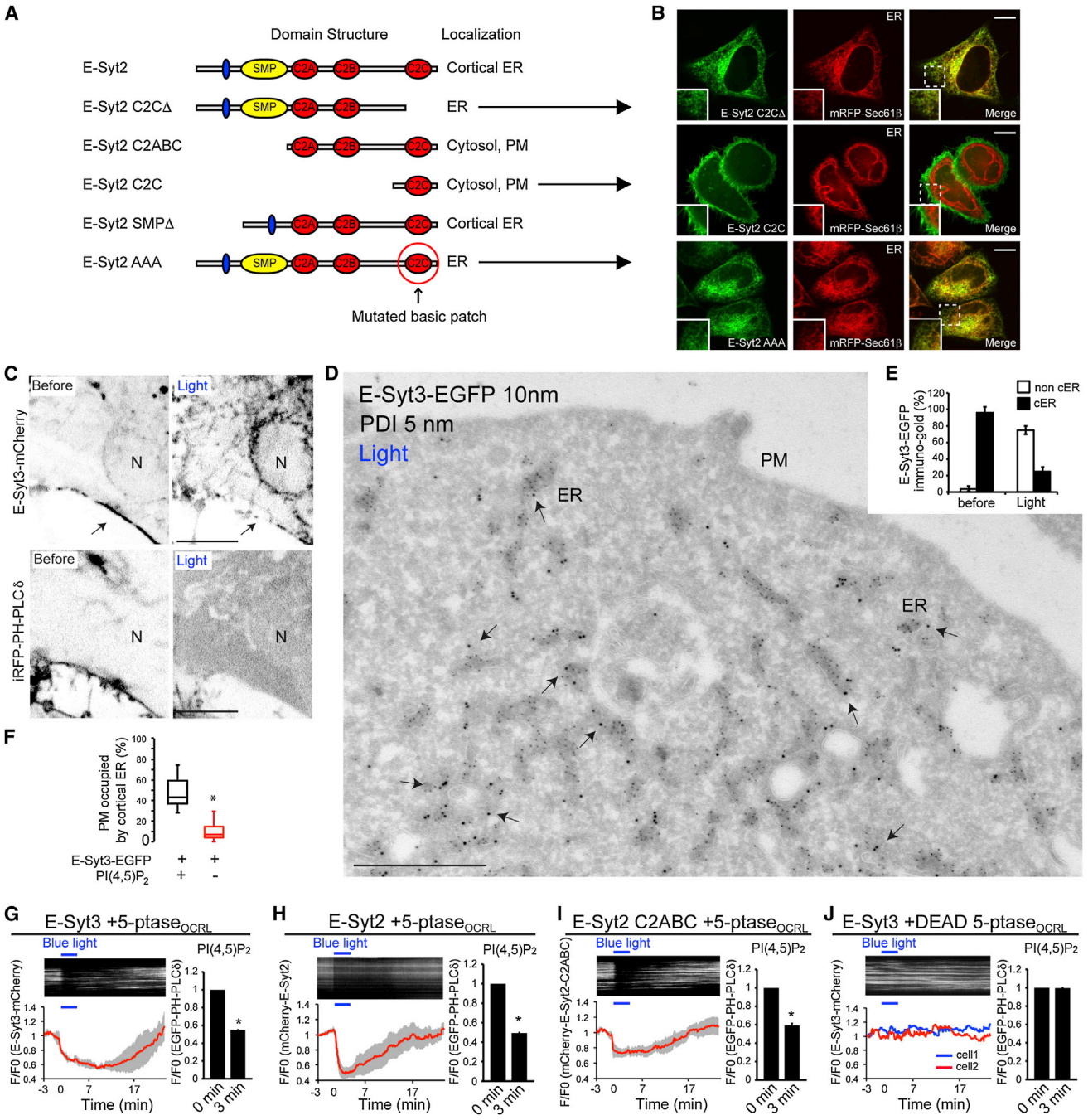

Figure 4. Interaction of the C2C Domains of E-Syt2/3 with PM PI(4,5)P_2 Is Required for the ER-PM Tethering Function of E-Syt2/3

(A) E-Syt2 constructs examined and their localizations.

(B) Confocal images of HeLa cells of constructs lacking the C2C domain or mutated in the basic patch in this domain. The C2C domain alone is targeted to the cell cortex. Scale bar, 10 μm.

(C) Confocal images of a COS-7 cell expressing E-Syt3-mCherry, the PI(4,5)P_2 reporter iRFP-PH-PLC$_{\delta1}$, and the two components of blue light-dependent PI(4,5)P_2 depletion system at the end of 10 min blue light illumination (arrow indicates cortical ER). Fluorescence is shown in black. N, nucleus. See also Movie S3. Scale bar, 5 μm.

(D–F) Immuno-EM micrograph (E-Syt3-EGFP, 10 nm gold and endogenous PDI, 5 nm gold) of cells processed as above and fixed at the end of the illumination. Quantification of the results is shown in (E) and (F). Note that the redistribution of E-Syt3-EGFP from cell periphery (cortical ER [cER]) (compare with Figure 1J) into the noncortical ER (arrows) is accompanied by loss of cER (mean ± SD) (F). The asterisk denotes $p < 0.001$.

(G–J) Time course of normalized mCherry fluorescence, as assessed by TIRF microscopy, from COS-7 cells expressing the indicated E-Syt fusion proteins together with EGFP-PH-PLC$_{\delta1}$ and the two components of blue light-dependent PI(4,5)P_2 depletion system (G)–(I) or the same two components but with a

(legend continued on next page)

CRY2-5-ptase$_{OCRL}$), (2) a PI(4,5)P_2 reporter (iRFP-PH-PLC$_{\delta1}$ or EFGP-PH-PLC$_{\delta1}$), and (3) either E-Syt2 or E-Syt3 constructs. Prior to illumination, robust signals for both E-Syt2 and E-Syt3 and the PI(4,5)P_2 reporter were detected in the cortical region of the cell by either total internal reflection fluorescence (TIRF) or confocal microscopy (arrows, Figures 4C, 4G, and 4H; Movie S3). Upon blue light illumination, the PI(4,5)P_2 reporter dissociated within seconds from the PM, consistent with PI(4,5)P_2 dephosphorylation (Figure 4C). This change correlated with a dispersion of E-Syt3 fluorescence from the cell periphery into the typical ER reticular network distributed throughout the cell, including the nuclear envelope (Figures 4C and 4G; Movie S3). Similar results were obtained for E-Syt2 (Figure 4H; Movie S4). The mCherry-tagged C2ABC region of E-Syt2 (Figure 4A) also relocated from the PM to the cytosol upon acute PI(4,5)P_2 depletion (Figure 4I). Both the relocation of the PI(4,5)P_2 reporter and of the E-Syts were reversible within minutes upon interruption of blue light illumination, likely due to PI(4,5)P_2 resynthesis (Idevall-Hagren et al., 2012). None of the effects described were elicited by a catalytically inactive mutant of the 5-phosphatase (Figure 4J).

Double immunogold labeling for E-Syt3-EGFP and for the lumenal ER marker PDI on ultrathin cryosections of cells fixed during exposure to blue light confirmed the massive redistribution of E-Syt3 (arrows, Figure 4D) from the cell periphery to the entire ER network (marked by PDI) (Figures 4D and 4E) and showed that this change was accompanied by 80% loss of cortical ER (Figure 4F). Additionally, TIRF microscopy imaging of E-Syt2-EGFP and a lumenal ER-marker (ER-mRFP) showed loss of both proteins from the cortical region of the cell during light-induced PI(4,5)P_2 depletion (Figure S3D), indicating loss of cortical ER structures.

Ca^{2+}-Dependent Recruitment of E-Syt1 to the PM

Several C2 domains bind phospholipid bilayers in a Ca^{2+}-dependent way. Inspection of the predicted structures of the C2 domains of the E-Syts revealed that amino acids required to confer Ca^{2+} binding are present in several of them and that both a Ca^{2+} binding site and an adjacent basic patch are present in the C2C domain of E-Syt1 (Fernandez et al., 2001) are most conserved in the C2C domain of E-Syt1 (Figure S4A). Thus, we asked whether recruitment of E-Syt1 to the cell cortex depends on elevation of cytosolic Ca^{2+}. Addition to cells expressing EGFP-E-Syt1 of 2 μM thapsigargin (TG), a drug that increases cytosolic Ca^{2+} by blocking its reuptake into the ER and by activating SOCE without major effects on PM PI(4,5)P_2 (Liou et al., 2005), resulted in the translocation of E-Syt1 to the cell cortex, as seen by both fluorescence microscopy (TIRF and confocal) and immuno-EM (Figures 5A–5D and S4B; Movie S5).

As this experiment did not exclude the possibility that E-Syt1 translocation requires ER Ca^{2+} depletion rather than cytosolic Ca^{2+} increase, the role of rapid cytosolic Ca^{2+} elevation was directly tested using Ca^{2+} uncaging. As shown by confocal microscopy, photolysis of caged Ca^{2+} in HeLa cells expressing mCherry-E-Syt1 induced a transient accumulation of this protein at the cell cortex, which was accompanied by the recruitment of the fluorescent ER lumenal marker ER-oxGFP (see Extended Experimental Procedures), reflecting formation of cortical ER (Figures 5F, left, and S4C; Movie S6). A lower amplitude increase of this signal was also observed in cells not expressing exogenous E-Syt1 (Figure S4C), indicating a physiological role of cytosolic Ca^{2+} in controlling dynamic ER-PM contacts and suggesting a potential role of endogenous E-Syt1 in these actions.

The translocation of E-Syt1, and correspondingly of the ER, to the PM in response to both thapsigargin and to Ca^{2+} uncaging was suppressed in cells where PM PI(4,5)P_2 was depleted by the optogenetic approach and also abolished by mutations in the C2C domain of E-Syt1 that disrupt its binding to Ca^{2+} (D663A, D675A, D722A, D724A, D726A, D728A, and D729A) (Figures 5E–5G). Thus, this redistribution most likely reflects Ca^{2+}-dependent PI(4,5)P_2 binding.

An interplay of cytosolic Ca^{2+} elevation and PM PI(4,5)P_2 was further demonstrated by another manipulation: stimulation of phospholipase C (PLC) by the muscarinic agonist oxotremorine M (Oxo-M) in cells overexpressing the muscarinic acetylcholine receptor. The increase in cytosolic Ca^{2+} produced by Oxo-M is triggered by inositol triphosphate, whose generation involves the consumption of PI(4,5)P_2. Thus, Ca^{2+}-dependent recruitment of E-Syt1 should be rapidly suppressed by the massive loss of PI(4,5)P_2 in the PM. Accordingly, an immediate, prominent, but only very transient recruitment of E-Syt1 and of the ER marker ER-oxGFP was produced by Oxo-M (Figures 5H and 7C).

Reciprocal Interactions of E-Syts

Members of the tricalbin/E-Syt family were reported to form dimers and multimers (Creutz et al., 2004; Groer et al., 2008; Jean et al., 2010). If E-Syt1 and E-Syt2/E-Syt3 interact, they may affect each other's localization. Supporting this possibility, when E-Syt1-EGFP was coexpressed with E-Syt2-mCherry or even more with E-Syt3-mCherry, an increase in the fraction of E-Syt1-EGFP located in cortical ER was observed both by fluorescence and by immunogold electron microscopy (Figures 6A–6C). Conversely, coexpression of E-Syt1 and E-Syt2 resulted in a substantial pool of E-Syt2 detectable throughout the ER. In agreement with the occurrence of a pool of E-Syt2 associated with E-Syt1 in noncortical ER, a small transient increase of E-Syt2-mCherry fluorescence was observed upon Oxo-M stimulation prior to the decrease due to PI(4,5)P_2 depletion, and this peak was abolished in cells when endogenous E-Syt1 expression was reduced by RNA interference (RNAi) (see below evidence for efficient RNAi-mediated E-Syt knockdown) (Figures 6D–6F). As expected, the muscarinic receptor antagonist atropine reversed these changes and even induced excess cortical accumulation of E-Syt2, a finding that was not further investigated. Conversely, in agreement with the presence of a

catalytically inactive phosphatase domain (DEAD 5-ptase$_{OCRL}$) (J). (Top) Kymographs of representative cells and (bottom) average traces (n = 5). Data are represented as mean ± SEM. The bar graphs on the right show levels of PI(4,5)P_2 as assessed by EGFP-PH-PLC$_{\delta1}$ fluorescence at time zero and at the end of the 3 min illumination. The asterisk denotes $p < 0.001$.
See also Figure S3 and Movies S3 and S4.

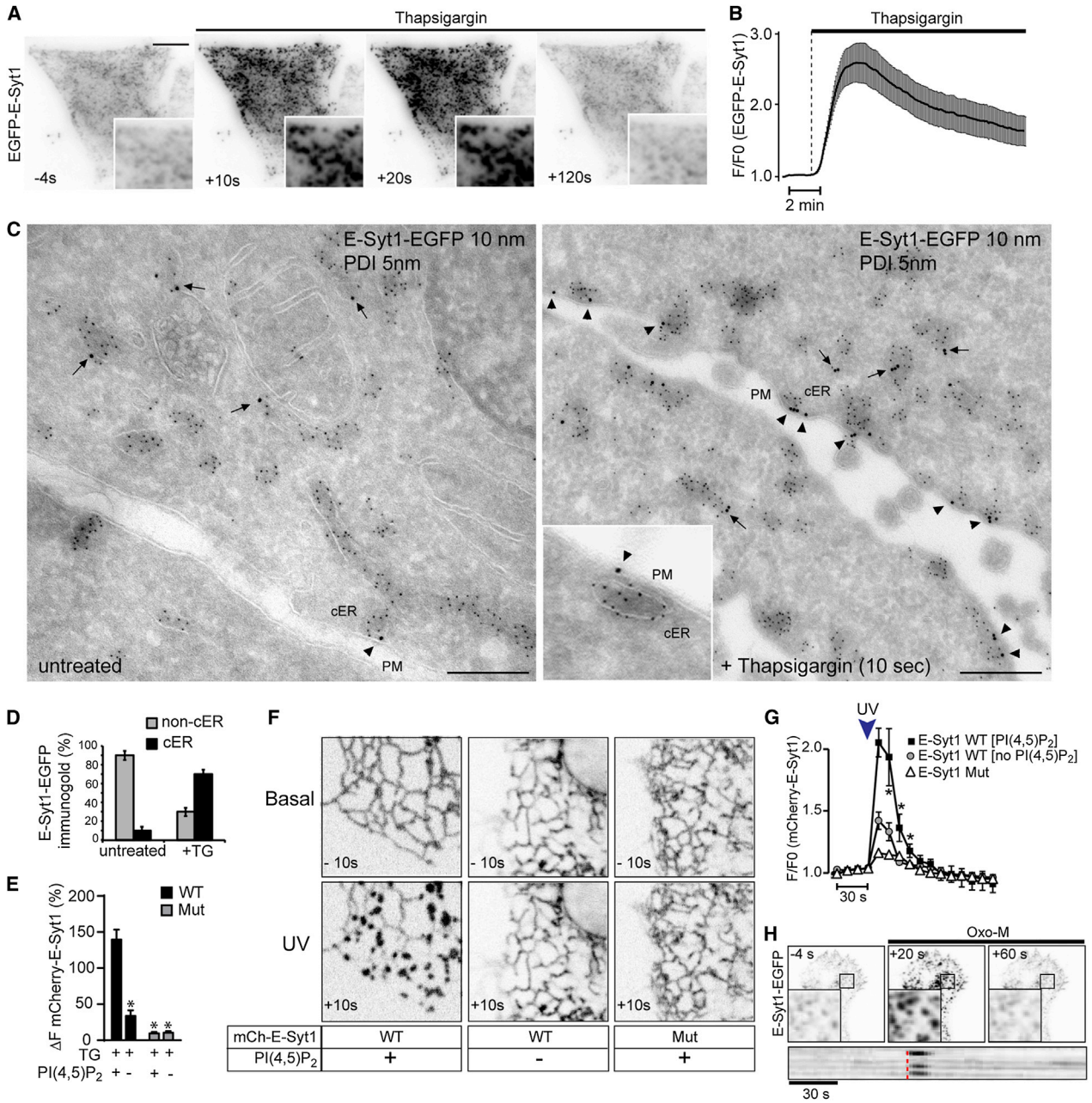

Figure 5. E-Syt1 Makes Dynamic Contacts with the PM in a Ca^{2+}- and $PI(4,5)P_2$-Dependent Manner

(A) TIRF microscopy images of a HeLa cell expressing EGFP-E-Syt1 before and after stimulation with 2 μM TG in the continued presence of extracellular Ca^{2+} at the indicated times. Scale bar, 10 μm.

(B) Time course of TG-induced recruitment of EGFP-E-Syt1 to the PM, as shown in (A) (mean ± SEM, n = 5).

(C) Immuno-EM micrographs of HeLa cells expressing E-Syt1-EGFP untreated or treated with TG (2 μM, 10 s). E-Syt1-EGFP (10 nm gold) and endogenous PDI (5 nm gold). Arrows indicate E-Syt1-positive noncortical ER, and arrowheads indicate E-Syt1-positive cortical ER (magnified in the inset). Scale bar, 200 nm.

(D) Quantification of the results in (C) (mean ± SD).

(E) Quantification of the response of wild-type (WT) or Ca^{2+}-binding deficient (Mut) mCherry-E-Syt1 to TG (2 μM, peak response) in HeLa cells, as assessed by TIRF microscopy with or without optogenetic depletion of PM $PI(4,5)P_2$ (mean ± SEM, n = 3 for each, *p < 0.001 for comparison to WT [TG]).

(F) Confocal images of the ventral region of COS-7 cells expressing WT or Mut mCherry-E-Syt1 before and 10 s after UV photolysis of caged Ca^{2+} with or without optogenetic depletion of PM $PI(4,5)P_2$. Hot spots of fluorescence represent focal accumulation of E-Syt1 at the PM.

(G) Time course of results shown in (F) (mean ± SEM, n = 7–15, *p < 0.01 compared to no $PI[4,5]P_2$).

(H) TIRF microscopy images of a HeLa cell expressing E-Syt1-EGFP and the M1R before and after stimulation with 10 μM Oxo-M. (Bottom) Kymograph of EGFP fluorescence of a representative cell. Fluorescence in (A), (F), and (H) is shown in black.

See also Figure S4 and Movies S5 and S6.

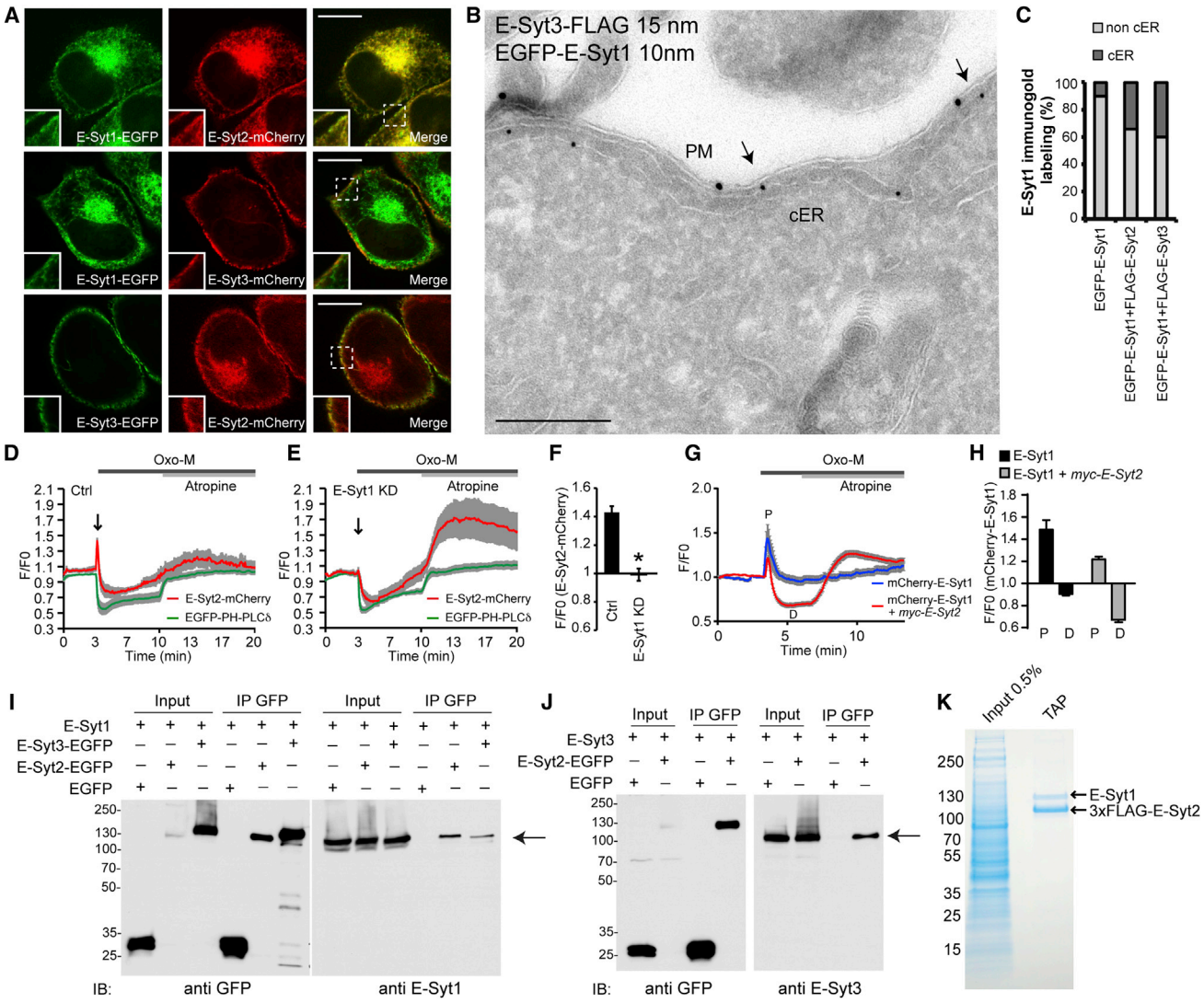

Figure 6. Heteromerization of the E-Syts

(A) Confocal images of HeLa cells coexpressing pairs of EGFP and mCherry E-Syts as indicated. Scale bar, 10 μm. Insets show at higher magnification of the areas framed by a dotted line.

(B) Immuno-EM micrograph of HeLa cells coexpressing E-Syt3-FLAG (15 nm gold) and EGFP-E-Syt1 (10 nm gold and arrows). Scale bar, 200 nm.

(C) Quantification of immunogold labeling for E-Syt1 on the noncortical portion of the ER (non-cER) and at ER-PM contact sites (cER) of cells expressing EGFP-E-Syt1 alone or together with 3xFLAG-E-Syt2 or E-Syt3-MycFLAG. Data are represented as mean.

(D and E) Time course of normalized mCherry and EGFP fluorescence, as assessed by TIRF microscopy, from HeLa cells expressing E-Syt2-mCherry and EGFP-PH-PLC$_{\delta 1}$ together with M1R. Cells were treated with either control siRNA (D) or siRNA specific for E-Syt1 (E) and stimulated with Oxo-M (10 μM), followed by addition of atropine (50 μM), as indicated (mean ± SEM).

(F) Quantification of fluorescence corresponding to the peak of E-Syt2 recruitment (arrows in the traces of [D] and [E]) (mean ± SEM; *$p < 0.001$).

(G and H) Time course of normalized mCherry fluorescence (TIRF) from HeLa cells expressing mCherry-E-Syt1 alone or together with Myc-E-Syt2. (H) Quantification of fluorescence corresponding to peak (P) and drop (D) in the traces of (G) (mean ± SEM).

(I and J) Extracts of HeLa cells transfected with the constructs indicated were subjected to anti-GFP immunoprecipitation (IP) and then processed for SDS-PAGE and immunoblotting (IB) with anti-GFP, anti-E-Syt1 (I), or anti-E-Syt3 (J) antibodies. Arrows indicate the coimmunoprecipitated bands. Inputs are 2.5% of the total cell lysates.

(K) Lysates of HeLa cells expressing EGFP-TEV-3xFLAG-E-Syt2 were tandem affinity purified using anti-GFP and anti-FLAG antibodies. Colloidal blue staining of gels of the starting extract (0.5%) and of the affinity-purified material is shown.

See also Figure S5.

pre-existing E-Syt1 pool at the cell cortex in cells coexpressing E-Syt1 and E-Syt2, the transient peak of mCherry-E-Syt1 signal observed by TIRF microscopy upon Oxo-M stimulation was lower than in cells where E-Syt1 was expressed alone, and a reduction of fluorescence relative to the prestimulation level was observed after this peak, consistent with loss of cortical

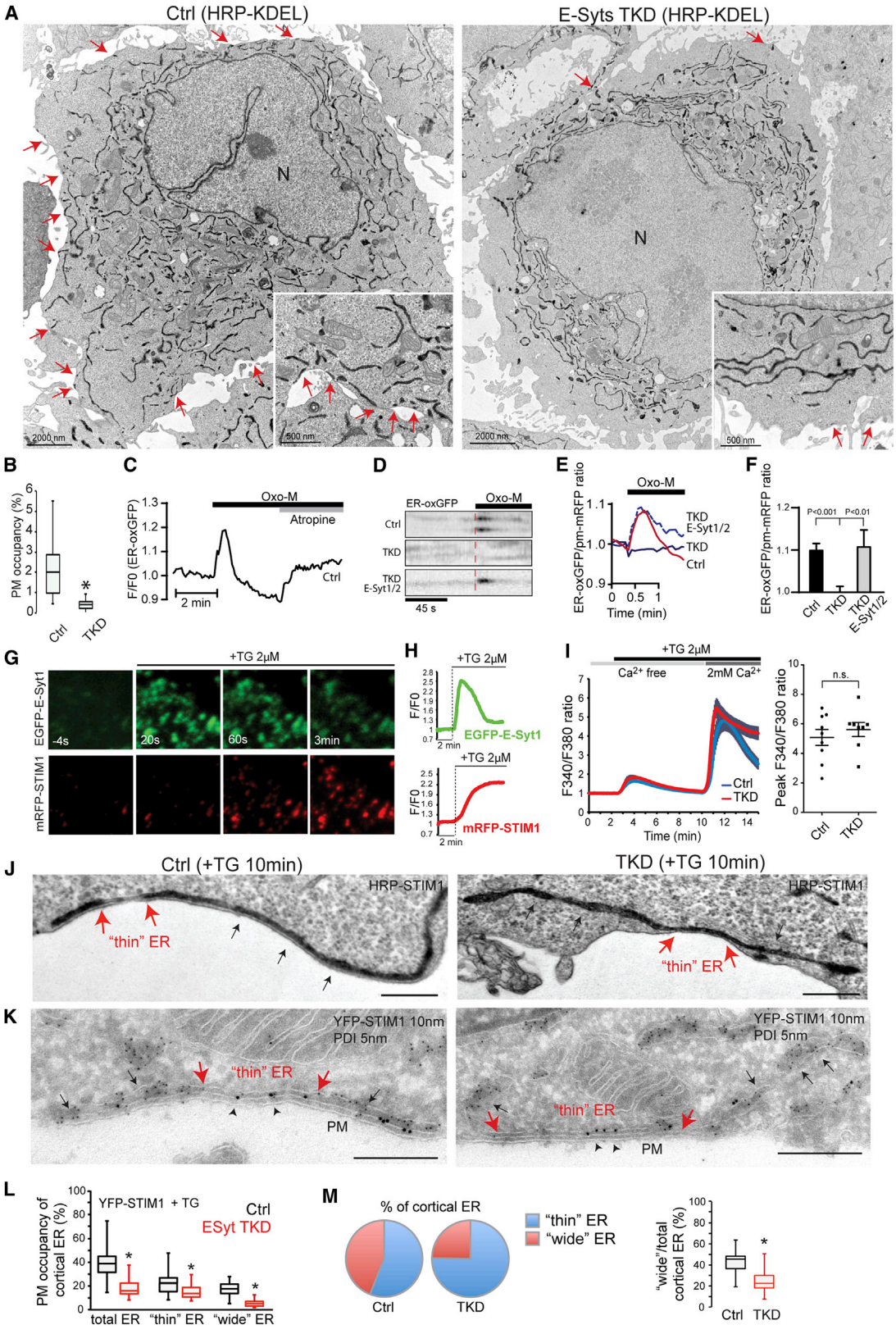

(legend on next page)

E-Syt2 upon PI(4,5)P_2 depletion (Figures 6G and 6H). Once again, the Oxo-M antagonist, atropine, reverted these changes to normal levels.

Formation of E-Syt complexes was supported by biochemical experiments. The presence of untagged E-Syts in immunoprecipitates from extracts of cells doubly transfected with EGFP-tagged and Myc-tagged forms of each E-Syt demonstrated homomerization (Figure S5A). Likewise, the presence of untagged E-Syt1 in anti-EGFP immunoprecipitates from cells cotransfected with this protein and with E-Syt2-EGFP or E-Syt3-EGFP and of untagged E-Syt2 or E-Syt3 in cells cotransfected with these proteins and with E-Syt1-EGFP (arrows, Figures 6I, 6J, and S5B) demonstrated that E-Syt2/E-Syt3 and E-Syt1 heterodimerize or heteromultimerize. Coomassie-blue-stained SDS-PAGE gel analysis of *t*andem *a*ffinity *p*urification (TAP)-tagged E-Syt2 (EGFP-tobacco etch virus [TEV]-3xFLAG-E-Syt2) immunoprecipitates confirmed robust complex formation of E-Syt2 with an endogenous protein identified by mass spectrometry as E-Syt1 (Figure 6K).

E-Syt Triple Knockdown Reduces ER-PM Contact Sites and Their Expansion in the Response to Cytosolic Ca^{2+} Elevations

The results reported so far show that the E-Syts can tether the ER to the PM. To test their requirement for ER-PM contacts, their expression was reduced by RNAi in HeLa cells. Robust suppression of all isoforms was confirmed by real-time quantitative PCR (qPCR) and by western blotting for E-Syt1 and E-Syt2 (E-Syt3 was undetectable in HeLa cells by western blotting, due to low expression levels) (Figures S6A–S6C).

Triple knockdown (TKD) of all E-Syts resulted in significant reduction (~50%) of the ER-oxGFP signal visible by TIRF microscopy (representing close ER-PM appositions) (Figures S6D and S6E), and this phenotype was rescued by coexpression of untagged small interfering RNA (siRNA)-resistant E-Syt1 and E-Syt2 (Figure S6E). At the EM level, ER-PM contacts, visualized by the electron dense reaction product in the ER of cells transfected with ssHRP-KDEL, decorated about 2% of the PM perimeter in control cells but only about 0.5% in TKD cells (Figures 7A and 7B).

Knockdown of the three E-Syts also impaired the Ca^{2+}-induced increase of ER-PM appositions. In control cells expressing ER-oxGFP and the muscarinic G protein-coupled receptor, addition of Oxo-M resulted in rapid and transient recruitment of the ER marker to the cell surface, which was seen as the appearance of fluorescent puncta visualized by TIRF microscopy. This recruitment was abolished in TKD cells and restored upon expression of untagged E-Syt1 and E-Syt2 (Figures 7C–7F). Thus, the E-Syts regulate not only the formation of ER-PM contacts but also the expansion of these contacts in a cytosolic Ca^{2+}-regulated way.

E-Syts Knockdown Does Not Affect SOCE

Given the critical role of ER-PM contacts in SOCE mediated by STIM1-Orai1 (Cahalan, 2009; Hogan et al., 2010), we asked whether the E-Syts have an impact on this system. In control conditions, STIM1 is broadly distributed throughout the ER, and its clustering upon Ca^{2+} depletion leads to its interaction with Orai1 in the PM, thus generating cortical ER (Wu et al., 2006). This cortical ER has a very narrow lumen ("thin" ER), possibly due to aggregation of the lumenal domain of STIM1, leading to exclusion of other ER proteins (Orci et al., 2009).

In untreated HeLa cells coexpressing mRFP-STIM1 and EGFP-E-Syt1, only weak E-Syt1 and STIM1 fluorescence was detectable in the TIRF field. Addition of TG in the presence of extracellular Ca^{2+} induced a punctate accumulation of both proteins at the cell cortex. The recruitment of EGFP-E-Syt1 due to cytosolic Ca^{2+} elevation occurred with faster kinetics and was transient, while the recruitment of mRFP-STIM1 due to depletion of Ca^{2+} from the ER lumen was slower (most likely reflecting, at

Figure 7. Knockdown of the E-Syts Decreases the Number of ER-PM Contacts but Does Not Impair SOCE

(A) EM micrographs of HRP-KDEL-expressing HeLa cells treated with control siRNA (Ctrl) or siRNAs against the three E-Syts (TKD). Red arrows indicate ER-PM contact sites. N, nucleus.

(B) The percentage of PM length engaged in contacts is shown as box and whisker plot (*$p < 0.001$).

(C) Time course of the normalized GFP signal, as assessed by TIRF microscopy, from a HeLa cell expressing a lumenal ER marker (ER-oxGFP) and M1R. Oxo-M (10 μM) stimulation and atropine (50 μM) addition are indicated.

(D–F) Dynamics of the cortical ER, as visualized by ER-oxGFP fluorescence in the TIRF field, in response to Oxo-M, in control or TKD cells coexpressing the PM marker pm-mRFP and M1R. For rescue, TKD cells were transfected with RNAi-resistant E-Syt1 and E-Syt2. Representative kymographs of the GFP fluorescence (black) and time course of the normalized ER-oxGFP/pm-mRFP ratios are shown in (D) and (E), respectively. (F) Quantification of fluorescence corresponding to the peaks in (E) (mean ± SEM, n = 3–10 for each condition).

(G) TIRF microscopy images of HeLa cells coexpressing EGFP-E-Syt1 and mRFP-STIM1 before and after the addition of TG (2 μM).

(H) Time course of the recruitment of EGFP-E-Syt1 (top) and mRFP-STIM1 (bottom) to the PM.

(I) Fura-2 Ca^{2+}-recordings of control and TKD cells. (Left) Time course of the normalized F340/F380 ratios of cells exposed to TG (2 μM) in Ca^{2+}-free medium, followed by Ca^{2+} add-back. The first response corresponds to Ca^{2+} leak from the ER, while the second response corresponds to Ca^{2+} entry from the extracellular medium (SOCE). (Right) SOCE peak values (mean ± SEM; n = 9 (Ctrl) and n = 8 (TKD); n.s., not significant).

(J) EM micrographs of control and TKD cells expressing HRP-STIM1 (dark staining) show cER upon treatment with TG (2 μM). Red arrows delimitate cER with a thin lumen. Black arrows indicate "wide" lumen.

(K) Immuno-EM micrographs of TG (2 μM) treated control and TKD cells transfected with YFP-STIM1 (anti-GFP, 10 nm gold) (arrowheads). Note the exclusion of PDI (5 nm gold) (black arrows) from the thin ER (delimited by red arrows) that is preserved in TKD cells. Scale bar, 250 nm.

(L) The percentages of PM length in EM sections, which is lined by the cortical ER (total) and by the thin and wide portions of such ER, are shown as box and whisker plot (*$p < 0.001$).

(M) (Left) Pie graphs showing the percentages of the thin and the wide lumen cER. (Right) Box and whisker plot showing that the relative proportion of the wide lumen cER is preferentially decreased in TKD cells (*$p < 0.001$).

See also Figure S6.

least in part, aggregation prior to recruitment) and persistent (Figures 7G and 7H).

TIRF microscopy-based quantitative analysis of mRFP-STIM1 recruitment to the cell periphery upon TG treatment showed a reduction (~50%) (Figure S6F) after RNAi-mediated E-Syt TKD, which could be at least partially explained by a global reduction in the proximity of the ER to the PM in the absence of the E-Syts because a large pool of STIM1 remains localized to the noncortical ER, even after ER Ca^{2+} depletion (Orci et al., 2009; Wu et al., 2006). However, in TKD cells, robust bright spots of colocalized mRFP-STIM1 and Orai1-EGFP still occurred in the TIRF field upon TG-dependent Ca^{2+} store depletion, although the total area occupied by these spots, as well as their number, was reduced (Figures S6G–S6I). Furthermore, no significant changes in the rise or peak value of SOCE, as detected by Fura-2, were observed in response to TG treatment in TKD cells (Figure 7I), indicating that E-Syts are not rate-limiting for this process. Only the clearance of cytosolic Ca^{2+} after the peak appeared to be delayed, a finding that we have not further investigated.

To gain insight into the lack of an impact of E-Syt TKD on SOCE (at least under the conditions tested), the architecture of ER-PM contacts sites after TG treatment was examined by EM. Ultrastructural analysis, including immunogold labeling, of cells expressing HRP-STIM1 (which broadly labels the ER lumen, even after a pool of STIM1 has been recruited to ER-PM contact sites) or yellow fluorescent protein (YFP)-STIM1 confirmed a reduction of cortical ER following TG treatment in TKD cells (Figures 7J–7L). Importantly, analysis of these samples revealed that this reduction involved predominantly wide ER structures, while thin cortical ER, where anti-YFP immunogold was concentrated and lumenal ER proteins were excluded (anti-PDI immunogold), was less affected (Figures 7J–7M). The presence of abundant thin ER, even in E-Syt TKD cells, may explain the persistence of efficient SOCE.

DISCUSSION

Our results demonstrate that all three E-Syts are resident proteins of the ER and that they function as regulated tethers between the ER and the PM. The interaction of the E-Syts with the PM is mediated by their C2 domains and requires PM $PI(4,5)P_2$, providing another example of the different contexts in which C2 domains are used to tether proteins or organelles to the PM (Figure S6J). In the case of E-Syt2 and E-Syt3, strong binding to the PM occurs at resting Ca^{2+} levels. In contrast, E-Syt1 binding to the PM is triggered by elevation of cytosolic Ca^{2+}, thus mediating or contributing to increased ER-PM appositions in response to Ca^{2+} rise. Interestingly, the C2A domain of E-Syt2 was shown to bind phospholipids in a Ca^{2+}-dependent way, but this interaction did not require acidic phospholipids (Min et al., 2007). Perhaps Ca^{2+} regulates the interaction of this domain "in cis" to the ER membrane, which is not enriched in acidic phospholipids. The requirement of $PI(4,5)P_2$ for E-Syts binding does not rule out additional roles of protein-binding partners in the PM. $PI(4,5)P_2$ may simply act as a critically required coreceptor, as shown for many other interactions involving phosphoinositides (Di Paolo and De Camilli, 2006). As the E-Syts homo- and heteromerize, the different properties of E-Syts present in heteromeric complexes may regulate and fine-tune their tethering functions and the functions of the tethers.

The other well-documented housekeeping mechanism responsible for regulated ER-PM contact formation, the STIM1-Orai1 system, is also dependent on changes in intracellular Ca^{2+}. However, STIM1-Orai1 contacts form in response to a loss of intralumenal Ca^{2+} in the ER, rather than to an increase in cytosolic Ca^{2+} (Cahalan, 2009; Hogan et al., 2010). As we have shown here, formation of STIM1-Orai1 contacts, corresponding to thin cortical ER in EM sections (Orci et al., 2009), also occurs in the absence of the E-Syts, although less prominently. Accordingly, robust SOCE occurs also in the absence of the E-Syts, when the global numbers or ER-PM contacts are decreased. These results indicate that E-Syts and STIM1-Orai1 represent independent ER-PM crosstalk systems.

Because some ER-PM contacts persist even when the expression levels of E-Syts are greatly reduced, other in trans interactions between the ER and the PM are expected to occur. This is consistent with studies in yeast, where the STIM1-Orai1 system is not present and where lack of the tricalbins alone resulted in a reduction, but not in a complete loss of cortical ER (Manford et al., 2012).

The localization of the E-Syts in the ER, an organelle that does not fuse with the plasma membrane, indicates that, although their overall domain organization is similar to that of the synaptotagmins, their function is fundamentally different. The synaptotagmins are localized in post-Golgi membranes and are implicated in tethering functions leading to exocytic fusion and in Ca^{2+}-dependent fusion itself (Südhof, 2012). This difference is further emphasized by the different topology in the membrane of the two protein families: synaptotagmins are conventional type I transmembrane proteins with a single transmembrane span and the N terminus in the noncytosolic space (Kida et al., 2005; Matteoli et al., 1992). In contrast, our data show that the bilayer anchoring stretch of the E-Syts forms a hairpin in the ER membrane so that their N terminus, like the bulk of the protein with the SMP and C2 domains, is in the cytosol. Interestingly, hairpin insertion in the membrane bilayer has been reported for several other ER proteins, including receptor expression-enhancing protein (REEP), the reticulons (Voeltz et al., 2006), spastin, and atlastins (Park et al., 2010). The previously reported accessibility of the N terminus of the E-Syt2 and E-Syt3 to the extracellular space, which had supported their PM localization, was obtained with cells that were fixed prior to immunostaining (Min et al., 2007), a condition that can result in loss of integrity of the PM. Our conclusions are consistent with other data of the study by Min et al. (2007) such as evidence for the importance of the C2C domains of E-Syt2 and E-Syt3 for their cortical targeting. We cannot rule out that a very small pool of E-Syts may end up in the PM, similar to what is the case of the ER protein STIM1 (Hewavitharana et al., 2008).

In spite of these differences, the property of the E-Syts to tether an intracellular membrane to the PM via C2-dependent interactions with acidic phospholipids is reminiscent of the property of Syt1 to tether secretory vesicles to the PM. Even in the case of Syt1, Ca^{2+}-independent and Ca^{2+}-dependent interactions cooperate, with Ca^{2+}-dependent interactions playing a role in Ca^{2+}-triggered secretory vesicle fusion (Chapman,

2008; Südhof, 2002, 2012). The presence in the E-Syts of an SMP domain, which is predicted to harbor a lipid within a hydrophobic grove (Kopec et al., 2010), and the observation, further supported by this study, that SMP domains are typically found in protein complexes that tether two membranes (Kornmann et al., 2009; Michel and Kornmann, 2012; Toulmay and Prinz, 2012) have suggested a role of the E-Syts/tricalbins in lipid transfer between the ER and the PM. If further studies validate this hypothesis, it will be of interest to determine how this function is regulated by Ca^{2+}.

In conclusion, our study identifies E-Syts/tricalbins as mediators of ER-PM contact sites and reveals mechanistic and dynamic aspects of these contacts. The conservation of the E-Syt/tricalbin family from yeast to mammals (Manford et al., 2012; Toulmay and Prinz, 2012) emphasizes the general importance of ER-PM contact sites in all eukaryotic cells, irrespective of the very different architecture of the ER in yeast and in higher eukaryotes and of the specialized role of a subset of these junctions, such as the ones involved in the control of Ca^{2+} entry, in animal cells. The characterization of the tricalbin/E-Syt protein family represents a starting point for a precise elucidation of the conserved and most fundamental molecular machinery that controls the crosstalk between the ER and the PM, onto which new functions have been superimposed during evolution to higher eukaryotes.

EXPERIMENTAL PROCEDURES

Full details are provided in the Extended Experimental Procedures.

Cell Culture, Transfection, and RNA Interference

HeLa, COS-7, and SH-SY5Y cells were cultured in Dulbecco's modified Eagle's medium (DMEM) containing 10% fetal bovine serum (FBS) at 37°C and 5% CO_2. Transfection of plasmids and RNAi oligos was carried out with Lipofectamine 2000 and RNAi MAX (Life Technologies).

Fluorescence Microscopy and Optogenetics

Spinning disc confocal (SDC) and TIRF microscopy were carried out as described in the Extended Experimental Procedures. For optogenetic control of PM $PI(4,5)P_2$, cells were transfected with heterodimerization modules that allow PM recruitment of an inositol-5-phosphatase catalytic domain upon blue light (488 nm) illumination as in Idevall-Hagren et al. (2012).

Ca^{2+} Uncaging

COS-7 cells were loaded with 10 μM o-nitrophenyl EGTA-AM (Life Technologies) in imaging buffer for 30 min at 37°C. Cells were subsequently washed twice and imaged on a SDC microscope. Photolysis of Ca^{2+} was achieved by a 3 s 405 nm light pulse.

Calcium Imaging

HeLa cells were loaded with 5 μM Fura-2-AM with Pluronic F127 (Invitrogen) in Ca^{2+}-containing buffer for 1 hr at room temperature. Cells were then washed twice and incubated with Ca^{2+}-free buffer before imaging. Thapsigargin (2 μM) (Life Technologies) was added in Ca^{2+}-free buffer, and Ca^{2+}-containing buffer was added back after Ca^{2+} store depletion.

Antibody Accessibility Assays and FPP Assay

To detect cell surface epitopes, live HeLa cells or SH-SY5Y cells cotransfected with Myc-Syt1 or Myc-E-Syts and mRFP-Sec61β were cooled to 4°C and incubated at 4°C with anti-Myc antibodies without fixation (nonpermeabilized conditions). Cells were then washed and fixed with 4% paraformaldehyde (PFA)/PBS and incubated with Alexa Fluor 488-conjugated anti-rabbit secondary antibody. After further washing, cells were examined with a SDC microscope. As a control, standard immunofluorescence of fixed and permeabilized cells was carried out. To detect cytosolically exposed epitopes on the ER membrane, live HeLa cells expressing Myc-tagged proteins were washed with potassium 4-(2-hydroxyethyl)-1-piperazineethanesulfonic acid magnesium (KHM) buffer, followed by KHM buffer containing 20 μM digitonin together with anti-Myc Alexa Fluor 488-conjugated antibody. Cells were incubated at room temperature for 5 min, washed with KHM buffer, and fixed with 4% PFA/KHM before imaging with a SDC microscope. Fluorescent protease protection (FPP) assay was carried out as described previously (Lorenz et al., 2006).

Electron Microscopy

Conventional EM, including HRP cytochemistry, and immunogold labeling of ultrathin frozen sections were performed according to standard procedures (Giordano et al., 2009). EM sections were observed under a Philips CM10 microscope equipped with a Morada 2k × 2k charge-coupled device (CCD) camera (Olympus).

Biochemical Analysis

For immunoprecipitation of GFP-tagged E-Syts, cell lysates were incubated with Chromotek GFP-trap agarose beads (Allele Biotech), and solubilized bead-bound material was processed for SDS-PAGE and immunoblotting. Tandem affinity purification of EGFP-TEV-3xFLAG-E-Syt2 and the cell-free translation/translocation assay are described in Extended Experimental Procedures.

Statistical Analysis

Comparisons of data were carried out using Student's t test.

SUPPLEMENTAL INFORMATION

Supplemental Information includes Extended Experimental Procedures, six figures, and six movies and can be found with this article online at http://dx.doi.org/10.1016/j.cell.2013.05.026.

ACKNOWLEDGMENTS

We thank Scott Emr (Cornell University) for his critical input in this work with discussion of unpublished data. We also thank Frank Wilson for outstanding technical support; Abel Alcazar-Roman for discussion and help; Heather Czapla, Yumei Wu, Morven Graham, Xinran Liu, and Stacy Wilson for help with microscopy experiments; Nicholas Ingolia (Carnegie Institution for Science) for consultation; and Thomas Südhof (Stanford University), Richard S. Lewis (Stanford University), Volker Haucke (Leibniz Institute, Berlin), Erik Snapp (Albert Einstein College of Medicine), Isabelle Derre, and Herve Agaisse (Yale University) for the generous gift of reagents, including unpublished reagents. We also acknowledge the Yale Center for Cellular and Molecular Imaging and Yale Center for Genomics and Proteomics. This work was supported in part by grants from the NIH (NS36251, DK082700, DK45735, and DA018343) and the Simons Foundation to P.D.C., the Italian Association for Cancer Research (AIRC grant IG9040) to N.B., fellowships from the Uehara Memorial Foundation and the Japan Society for Promotion and Science to Y.S., and the Swedish Research Council to O.I.-H.

Received: March 11, 2013
Revised: April 24, 2013
Accepted: May 10, 2013
Published: June 20, 2013

REFERENCES

Anderie, I., Schulz, I., and Schmid, A. (2007). Characterization of the C-terminal ER membrane anchor of PTP1B. Exp. Cell Res. *313*, 3189–3197.

Block, B.A., Imagawa, T., Campbell, K.P., and Franzini-Armstrong, C. (1988). Structural evidence for direct interaction between the molecular components

of the transverse tubule/sarcoplasmic reticulum junction in skeletal muscle. J. Cell Biol. *107*, 2587–2600.

Brambillasca, S., Yabal, M., Soffientini, P., Stefanovic, S., Makarow, M., Hegde, R.S., and Borgese, N. (2005). Transmembrane topogenesis of a tail-anchored protein is modulated by membrane lipid composition. EMBO J. *24*, 2533–2542.

Cahalan, M.D. (2009). STIMulating store-operated Ca(2+) entry. Nat. Cell Biol. *11*, 669–677.

Chapman, E.R. (2008). How does synaptotagmin trigger neurotransmitter release? Annu. Rev. Biochem. *77*, 615–641.

Creutz, C.E., Snyder, S.L., and Schulz, T.A. (2004). Characterization of the yeast tricalbins: membrane-bound multi-C2-domain proteins that form complexes involved in membrane trafficking. Cell. Mol. Life Sci. *61*, 1208–1220.

Di Paolo, G., and De Camilli, P. (2006). Phosphoinositides in cell regulation and membrane dynamics. Nature *443*, 651–657.

Diril, M.K., Wienisch, M., Jung, N., Klingauf, J., and Haucke, V. (2006). Stonin 2 is an AP-2-dependent endocytic sorting adaptor for synaptotagmin internalization and recycling. Dev. Cell *10*, 233–244.

Elbaz, Y., and Schuldiner, M. (2011). Staying in touch: the molecular era of organelle contact sites. Trends Biochem. Sci. *36*, 616–623.

Endo, M. (2009). Calcium-induced calcium release in skeletal muscle. Physiol. Rev. *89*, 1153–1176.

Fernandez, I., Araç, D., Ubach, J., Gerber, S.H., Shin, O., Gao, Y., Anderson, R.G., Südhof, T.C., and Rizo, J. (2001). Three-dimensional structure of the synaptotagmin 1 C2B-domain: synaptotagmin 1 as a phospholipid binding machine. Neuron *32*, 1057–1069.

Feske, S., Gwack, Y., Prakriya, M., Srikanth, S., Puppel, S.H., Tanasa, B., Hogan, P.G., Lewis, R.S., Daly, M., and Rao, A. (2006). A mutation in Orai1 causes immune deficiency by abrogating CRAC channel function. Nature *441*, 179–185.

Franzini-Armstrong, C., and Jorgensen, A.O. (1994). Structure and development of E-C coupling units in skeletal muscle. Annu. Rev. Physiol. *56*, 509–534.

Friedman, J.R., and Voeltz, G.K. (2011). The ER in 3D: a multifunctional dynamic membrane network. Trends Cell Biol. *21*, 709–717.

Giordano, F., Bonetti, C., Surace, E.M., Marigo, V., and Raposo, G. (2009). The ocular albinism type 1 (OA1) G-protein-coupled receptor functions with MART-1 at early stages of melanogenesis to control melanosome identity and composition. Hum. Mol. Genet. *18*, 4530–4545.

Groer, G.J., Haslbeck, M., Roessle, M., and Gessner, A. (2008). Structural characterization of soluble E-Syt2. FEBS Lett. *582*, 3941–3947.

Hewavitharana, T., Deng, X., Wang, Y., Ritchie, M.F., Girish, G.V., Soboloff, J., and Gill, D.L. (2008). Location and function of STIM1 in the activation of Ca2+ entry signals. J. Biol. Chem. *283*, 26252–26262.

Higy, M., Junne, T., and Spiess, M. (2004). Topogenesis of membrane proteins at the endoplasmic reticulum. Biochemistry *43*, 12716–12722.

Hogan, P.G., Lewis, R.S., and Rao, A. (2010). Molecular basis of calcium signaling in lymphocytes: STIM and ORAI. Annu. Rev. Immunol. *28*, 491–533.

Holthuis, J.C., and Levine, T.P. (2005). Lipid traffic: floppy drives and a superhighway. Nat. Rev. Mol. Cell Biol. *6*, 209–220.

Idevall-Hagren, O., Dickson, E.J., Hille, B., Toomre, D.K., and De Camilli, P. (2012). Optogenetic control of phosphoinositide metabolism. Proc. Natl. Acad. Sci. USA *109*, E2316–E2323.

Jean, S., Mikryukov, A., Tremblay, M.G., Baril, J., Guillou, F., Bellenfant, S., and Moss, T. (2010). Extended-synaptotagmin-2 mediates FGF receptor endocytosis and ERK activation in vivo. Dev. Cell *19*, 426–439.

Kida, Y., Mihara, K., and Sakaguchi, M. (2005). Translocation of a long amino-terminal domain through ER membrane by following signal-anchor sequence. EMBO J. *24*, 3202–3213.

Kopec, K.O., Alva, V., and Lupas, A.N. (2010). Homology of SMP domains to the TULIP superfamily of lipid-binding proteins provides a structural basis for lipid exchange between ER and mitochondria. Bioinformatics *26*, 1927–1931.

Kornmann, B., Currie, E., Collins, S.R., Schuldiner, M., Nunnari, J., Weissman, J.S., and Walter, P. (2009). An ER-mitochondria tethering complex revealed by a synthetic biology screen. Science *325*, 477–481.

Lee, I., and Hong, W. (2006). Diverse membrane-associated proteins contain a novel SMP domain. FASEB J. *20*, 202–206.

Levine, T., and Loewen, C. (2006). Inter-organelle membrane contact sites: through a glass, darkly. Curr. Opin. Cell Biol. *18*, 371–378.

Lewis, R.S. (2007). The molecular choreography of a store-operated calcium channel. Nature *446*, 284–287.

Liou, J., Kim, M.L., Heo, W.D., Jones, J.T., Myers, J.W., Ferrell, J.E., Jr., and Meyer, T. (2005). STIM is a Ca2+ sensor essential for Ca2+-store-depletion-triggered Ca2+ influx. Curr. Biol. *15*, 1235–1241.

Lorenz, H., Hailey, D.W., Wunder, C., and Lippincott-Schwartz, J. (2006). The fluorescence protease protection (FPP) assay to determine protein localization and membrane topology. Nat. Protoc. *1*, 276–279.

Manford, A.G., Stefan, C.J., Yuan, H.L., Macgurn, J.A., and Emr, S.D. (2012). ER-to-plasma membrane tethering proteins regulate cell signaling and ER morphology. Dev. Cell *23*, 1129–1140.

Matteoli, M., Takei, K., Perin, M.S., Südhof, T.C., and De Camilli, P. (1992). Exo-endocytotic recycling of synaptic vesicles in developing processes of cultured hippocampal neurons. J. Cell Biol. *117*, 849–861.

Michel, A.H., and Kornmann, B. (2012). The ERMES complex and ER-mitochondria connections. Biochem. Soc. Trans. *40*, 445–450.

Min, S.W., Chang, W.P., and Südhof, T.C. (2007). E-Syts, a family of membranous Ca2+-sensor proteins with multiple C2 domains. Proc. Natl. Acad. Sci. USA *104*, 3823–3828.

Orci, L., Ravazzola, M., Le Coadic, M., Shen, W.W., Demaurex, N., and Cosson, P. (2009). From the Cover: STIM1-induced precortical and cortical subdomains of the endoplasmic reticulum. Proc. Natl. Acad. Sci. USA *106*, 19358–19362.

Park, S.H., Zhu, P.P., Parker, R.L., and Blackstone, C. (2010). Hereditary spastic paraplegia proteins REEP1, spastin, and atlastin-1 coordinate microtubule interactions with the tubular ER network. J. Clin. Invest. *120*, 1097–1110.

Perin, M.S., Fried, V.A., Mignery, G.A., Jahn, R., and Südhof, T.C. (1990). Phospholipid binding by a synaptic vesicle protein homologous to the regulatory region of protein kinase C. Nature *345*, 260–263.

Porter, K.R., and Palade, G.E. (1957). Studies on the endoplasmic reticulum. III. Its form and distribution in striated muscle cells. J. Biophys. Biochem. Cytol. *3*, 269–300.

Rizo, J., and Südhof, T.C. (1998). C2-domains, structure and function of a universal Ca2+-binding domain. J. Biol. Chem. *273*, 15879–15882.

Rosenbluth, J. (1962). Subsurface cisterns and their relationship to the neuronal plasma membrane. J. Cell Biol. *13*, 405–421.

Schikorski, T., Young, S.M., Jr., and Hu, Y. (2007). Horseradish peroxidase cDNA as a marker for electron microscopy in neurons. J. Neurosci. Methods *165*, 210–215.

Schulz, T.A., Choi, M.G., Raychaudhuri, S., Mears, J.A., Ghirlando, R., Hinshaw, J.E., and Prinz, W.A. (2009). Lipid-regulated sterol transfer between closely apposed membranes by oxysterol-binding protein homologues. J. Cell Biol. *187*, 889–903.

Sharpe, H.J., Stevens, T.J., and Munro, S. (2010). A comprehensive comparison of transmembrane domains reveals organelle-specific properties. Cell *142*, 158–169.

Shen, W.W., Frieden, M., and Demaurex, N. (2011). Remodelling of the endoplasmic reticulum during store-operated calcium entry. Biol. Cell *103*, 365–380.

Shibata, Y., Voss, C., Rist, J.M., Hu, J., Rapoport, T.A., Prinz, W.A., and Voeltz, G.K. (2008). The reticulon and DP1/Yop1p proteins form immobile oligomers in the tubular endoplasmic reticulum. J. Biol. Chem. *283*, 18892–18904.

Stefan, C.J., Manford, A.G., Baird, D., Yamada-Hanff, J., Mao, Y., and Emr, S.D. (2011). Osh proteins regulate phosphoinositide metabolism at ER-plasma membrane contact sites. Cell *144*, 389–401.

Stefan, C.J., Manford, A.G., and Emr, S.D. (2013). ER-PM connections: sites of information transfer and inter-organelle communication. Curr. Opin. Cell Biol. Published online March 19, 2013. http://dx.doi.org/10.1016/j.ceb.2013.02.020.

Südhof, T.C. (2002). Synaptotagmins: why so many? J. Biol. Chem. *277*, 7629–7632.

Südhof, T.C. (2012). Calcium control of neurotransmitter release. Cold Spring Harb. Perspect. Biol. *4*, a011353.

Takeshima, H., Komazaki, S., Nishi, M., Iino, M., and Kangawa, K. (2000). Junctophilins: a novel family of junctional membrane complex proteins. Mol. Cell *6*, 11–22.

Toulmay, A., and Prinz, W.A. (2011). Lipid transfer and signaling at organelle contact sites: the tip of the iceberg. Curr. Opin. Cell Biol. *23*, 458–463.

Toulmay, A., and Prinz, W.A. (2012). A conserved membrane-binding domain targets proteins to organelle contact sites. J. Cell Sci. *125*, 49–58.

Voeltz, G.K., Prinz, W.A., Shibata, Y., Rist, J.M., and Rapoport, T.A. (2006). A class of membrane proteins shaping the tubular endoplasmic reticulum. Cell *124*, 573–586.

West, M., Zurek, N., Hoenger, A., and Voeltz, G.K. (2011). A 3D analysis of yeast ER structure reveals how ER domains are organized by membrane curvature. J. Cell Biol. *193*, 333–346.

Wu, M.M., Buchanan, J., Luik, R.M., and Lewis, R.S. (2006). Ca2+ store depletion causes STIM1 to accumulate in ER regions closely associated with the plasma membrane. J. Cell Biol. *174*, 803–813.

Zhang, S.L., Yu, Y., Roos, J., Kozak, J.A., Deerinck, T.J., Ellisman, M.H., Stauderman, K.A., and Cahalan, M.D. (2005). STIM1 is a Ca2+ sensor that activates CRAC channels and migrates from the Ca2+ store to the plasma membrane. Nature *437*, 902–905.